

The Super - Kamiokande Day - Night Effect Data and the MSW Solutions of the Solar Neutrino Problem

M. Maris^a and S.T. Petcov^{b,c)*}

a) Osservatorio Astronomico di Trieste, I-34113 Trieste, Italy

b) Scuola Internazionale Superiore di Studi Avanzati, I-34014 Trieste, Italy

c) Istituto Nazionale di Fizica Nucleare, Sezione di Trieste, I-34014 Trieste, Italy

Abstract

The current Super-Kamiokande data on the D-N asymmetry between the the day event rate and the *Night* (*Mantle*) and *Core* event rates, produced by solar neutrinos which respectively cross the Earth along any trajectory (cross the Earth mantle but do not cross the core), and cross the Earth core before reaching the detector, imply rather stringent constraints on the MSW small mixing angle (SMA) $\nu_e \rightarrow \nu_{\mu(\tau)}$ solution of the solar neutrino problem. A simplified analysis shows, in particular, that a substantial subregion of the SMA solution region is disfavored by these data. The *Core* D-N asymmetry data alone allow to rule out at 99.7% C.L. a part of this subregion. The constraints on the MSW large mixing angle and LOW $\nu_e \rightarrow \nu_{\mu(\tau)}$ solutions as well as on the MSW $\nu_e \rightarrow \nu_s$ solution, following from the data on the *Mantle*, *Night* and *Core* D-N asymmetries are also discussed.

*Also at: Institute of Nuclear Research and Nuclear Energy, Bulgarian Academy of Sciences, BG-1784 Sofia, Bulgaria.

I. Introduction: The MSW Solutions of the Solar Neutrino Problem and the Day-Night Effect

The hypothesis of MSW transitions of solar neutrinos continues to provide a viable solution of the solar neutrino problem [1–9]. The current (mean event rate) solar neutrino data admit three types of MSW $\nu_e \rightarrow \nu_{\mu(\tau)}$ transition solutions: the well-known small mixing angle (SMA) non-adiabatic and large mixing angle (LMA) adiabatic (see, e.g., [10,11]) and the so-called “LOW” solution (very recent analyses can be found in, e.g., [5,7–9]). While the SMA and LMA solutions have been shown to be rather stable with respect to variations in the values of the various physical quantities which enter into the calculations (the fluxes of ^8B and ^7Be neutrinos, nuclear reaction cross-sections, etc.), and of the data utilized in the analyses, the LOW solution is of the “borderline” type: its existence even at 99% C.L. is not stable with respect to relatively small changes in the data and/or in the relevant theoretical predictions (see, e.g., [7] and the references quoted therein.).

To the three solutions there correspond (at a given C.L.) three distinct regions in the plane of values of the two parameters, Δm^2 and $\sin^2 2\theta$, characterizing the transitions. One finds [5,7–9] using the standard solar model predictions [6] for the solar neutrino fluxes (^8B , ^7Be , pp , etc.) that at 99% C.L. the SMA MSW solution requires values in the intervals $4.0 \times 10^{-6} \text{ eV}^2 \lesssim \Delta m^2 \lesssim 10.0 \times 10^{-6} \text{ eV}^2$, $1.3 \times 10^{-3} \lesssim \sin^2 2\theta \lesssim 1.0 \times 10^{-2}$, the LMA solutions is realized for Δm^2 and $\sin^2 2\theta$ from the region $7.0 \times 10^{-6} \text{ eV}^2 \lesssim \Delta m^2 \lesssim 2.0 \times 10^{-4} \text{ eV}^2$, $0.50 \lesssim \sin^2 2\theta \lesssim 1.0$, and the LOW solution lies approximately in the region $0.4 \times 10^{-7} \text{ eV}^2 \lesssim \Delta m^2 \lesssim 1.5 \times 10^{-7} \text{ eV}^2$, $0.80 \lesssim \sin^2 2\theta \lesssim 1.0$. The SMA and LMA solution regions expand in the direction of smaller values of $\sin^2 2\theta$ up to $\sim 0.6 \times 10^{-3}$ and to ~ 0.3 , respectively, if one adopts a more *conservative* approach in analyzing the data in terms of the MSW effect and treats the ^8B neutrino flux as a free parameter in the analysis (see, e.g., [9]).

A unique testable prediction of the MSW solutions of the solar neutrino problem is the day-night (D-N) effect - a difference between the solar neutrino event rates during the day and during the night, caused by the additional transitions of the solar neutrinos taking place at night while the neutrinos cross the Earth on the way to the detector (see, e.g., [11,14] and the references quoted therein). The experimental observation of a non-zero D-N asymmetry

$$A_{D-N}^N \equiv \frac{R_N - R_D}{(R_N + R_D)/2}, \quad (1)$$

where R_N and R_D are, e.g., the one year averaged event rates in a given detector respectively during the night and the day, would be a very strong evidence in favor (if not a proof) of the MSW solution of the solar neutrino problem.

Extensive predictions for the magnitude of the D-N effect for the Super-Kamiokande detector have been obtained in [15–19]. Earlier results have been derived in [11,14]. High precision calculations of the D-N asymmetry in the one year averaged recoil- e^- spectrum and in the energy-integrated event rates were performed for three event samples, *Night*, *Core* and *Mantle*, in [15–17]. The night fractions of these event samples are due to neutrinos which respectively cross the Earth along any trajectory, cross the Earth core, and cross only the Earth mantle (but not the core), on the way to the detector. The measurement of the D-N asymmetry in the *Core* sample was found to be of particular importance [15,16] because of the strong enhancement of the asymmetry, caused by a constructive interference between the amplitudes of the neutrino transitions in the Earth mantle and in the Earth core [20]. The effect differs from the MSW one [20]. The *mantle-core enhancement effect* is caused by the existence (for a given neutrino trajectory through the Earth core) of *points of resonance-like total neutrino conversion* in the corresponding space of neutrino oscillation parameters [21,22]. The location of these points determines the regions where the relevant probability of transitions in the

Earth of the Earth-core-crossing solar neutrinos is large * [22]. At small mixing angles and in the case of $\nu_e \rightarrow \nu_{\mu(\tau)}$ transitions the predicted D-N asymmetry in the *Core* sample of the Super-Kamiokande event rate data was shown [16] to be much bigger due to the *mantle-core enhancement* effect [†] - by a factor of up to ~ 6 , than the asymmetry in the *Night* sample. The asymmetry in the *Mantle* sample was found to be smaller than the asymmetry in the *Night* sample. On the basis of these results it was concluded in [16] that it can be possible to test a substantial part of the MSW $\nu_e \rightarrow \nu_{\mu(\tau)}$ SMA solution region in the $\Delta m^2 - \sin^2 2\theta$ plane by performing selective, i.e., *Core* and *Night* (or *Mantle*) D-N asymmetry measurements.

The current Super-Kamiokande data [5] shows a D-N asymmetry in the *Night* sample, which is different from zero at 1.9 s.d. level:

$$A_{D-N}^N = 0.065 \pm 0.031 \text{ (stat.)} \pm 0.013 \text{ (syst.)}. \quad (2)$$

These data allow to probe only a relatively small subregion of the SMA “conservative” solution region: the predicted asymmetry is too small (see, e.g., [16,18,19]). However, the Super-Kamiokande night data is given in 5 bins and 80% of the events in the bin N5 are due to Earth-core-crossing solar neutrinos [5], while the remaining 20% are produced by neutrinos which cross only the Earth mantle. Since the predicted D-N asymmetry in the *Mantle* sample is practically negligible in the case of the MSW SMA solution of interest [16], we have for the D-N asymmetry measured using the night N5 bin data: $A_{D-N}^{N5} \cong 0.8 A_{D-N}^C$, A_{D-N}^C being the asymmetry in the *Core* sample. The data on A_{D-N}^{N5} [5] permitted to exclude a part of the MSW SMA solution region located in the area $\sin^2 2\theta \cong (0.007 - 0.01)$, $\Delta m^2 \cong (0.5 - 1.0) \times 10^{-5} \text{ eV}^2$. It should be obvious from the above discussion that the measurement of the *Core* asymmetry A_{D-N}^C , as suggested in [16], will provide a more effective test of the MSW SMA solution than the measurement of A_{D-N}^{N5} .

Recently the Super-Kamiokande collaboration for the first time published data on the *Core* D-N asymmetry A_{D-N}^C [23]:

$$A_{D-N}^C = -0.0175 \pm 0.0622 \text{ (stat.)} \pm 0.013 \text{ (syst.)}. \quad (3)$$

The experimental value of the *Mantle* asymmetry can also be deduced from the data [23]:

$$A_{D-N}^M = 0.0769 \pm 0.034 \text{ (stat.)} \pm 0.013 \text{ (syst.)}. \quad (4)$$

In the present article we use the Super-Kamiokande results on the D - N effect, eqs. (2), (3) and (4), to derive constraints on the MSW $\nu_e \rightarrow \nu_{\mu(\tau)}$ transition solutions of the solar neutrino problem. We show below, in particular, that, as has been suggested in [16], the data on the *Core* and *Night* or *Mantle* D - N asymmetries allow to perform a very effective test of the MSW SMA solution. We also obtain constraints on the MSW LMA and LOW $\nu_e \rightarrow \nu_{\mu(\tau)}$ solutions as well as on the MSW $\nu_e \rightarrow \nu_s$ solution, following from the Super-Kamiokande data on the *Mantle*, *Night* and *Core* D-N asymmetries.

* Being a constructive interference effect between the amplitudes of neutrino transitions in the mantle and in the core, this is not just “core enhancement” effect, but rather *mantle-core enhancement* effect.

[†]The term “neutrino oscillation length resonance” (NOLR) was used in [20], in particular, to denote the enhancement in this case.

II. Constraints on the MSW Solutions from the Super-Kamiokande Data on the *Core* and *Mantle* or *Night* Day-Night Asymmetries

We use the high precision methods of calculation of the energy-integrated one year average *Core*, *Night* and *Mantle* D-N asymmetries developed for our earlier studies of the D-N effect for the Super-Kamiokande detector, which are described in detail in [15–17]. The cross section of the $\nu_e - e^-$ elastic scattering reaction was taken from [24]. We used in our calculations the ^8B neutrino spectrum derived in [25]. The probability of survival of the solar ν_e when they travel in the Sun and further to the surface of the Earth, $\bar{P}_\odot(\nu_e \rightarrow \nu_e)$, was computed on the basis of the analytic expression obtained in [26] and using the method developed in [27]. In the calculation of $\bar{P}_\odot(\nu_e \rightarrow \nu_e)$ we have utilized (as in [15–17]) the density profile of the Sun and the ^8B neutrino production distribution in the Sun, predicted in [28]. These predictions were updated in [6], but a detailed test study showed [29] (see also [19]) that using the results of [6] instead of those in [28] leads to a change of the survival probability by less than 1% for any set of values of the parameters Δm^2 and $\sin^2 2\theta$, relevant for the calculation of the D-N effect. As in [15–17], the Earth matter effects were calculated using the Stacey model from 1977 [30] for the Earth density distribution. The latter practically coincides with that predicted by the more recent Earth model [31]. Our results are obtained for the standard values of the electron fraction number in the Earth mantle and the Earth core, $Y_e^{man} = 0.49$ and $Y_e^c = 0.467$, which reflect the chemical composition of the two major Earth structures (see, e.g., [32,16]).

In our simplified analysis we use the Super-Kamiokande data on the *Core* and *Mantle* or *Night* D-N asymmetries, treating the *Core* and *Mantle*, and the *Core* and *Night* asymmetries as two pairs of independent observables. While this is certainly justified in the case of the *Core* and *Mantle* asymmetries, the treatment of the *Core* and *Night* asymmetries neglects the possible (weak) correlation between the values of the two asymmetries. Note, however, that i) since such a correlation does not exist in the case of the *Core* and *Mantle* asymmetries and ii) the statistics in the *Night* sample of Super-Kamiokande events is dominated by that in the *Mantle* sample, we expect that the results obtained using the data on *Core* and *Night* asymmetries without taking into account the correlation between the two will not differ substantially from those derived by accounting for the correlation. The indicated results should not differ much also from those found by using the data on the *Core* and *Mantle* asymmetries. Actually, the restrictions following from the latter set of data turned out to be somewhat stronger than those derived by us on the basis of *Core* and *Night* asymmetry data.

The results of our study are presented graphically in Figs. 1a - 1c and 2a - 2c. In Figs. 1a - 1c (2a - 2c) the “conservative” MSW SMA (LMA and LOW) solution region in the $\Delta m^2 - \sin^2 2\theta$ plane of oscillation parameters is shown (grey area) together with the regions allowed by the Super-Kamiokande data on the *Core*, *Night* and *Mantle* D-N asymmetries at 1.0 s.d. (a), 1.5 s.d. (b) and 2.0 s.d. (c). The MSW solution regions were obtained [9] using the mean event rate solar neutrino data [1–5]. Contours of constant *Core* D-N asymmetry in the plane of the two parameters are also shown (thin solid lines), with the value of the asymmetry corresponding to a given contour indicated on the contour. The regions allowed by the *Core* asymmetry data in Figs. 1a - 1c are located to the left of the thick (black) solid line, while in Figs. 2a - 2c these regions are situated above the upper and below the lower thick (black) solid lines. The regions allowed by the *Night* asymmetry data in Figs. 1a - 1c are between the two dashed lines, in Figs. 2a - 2b they are between the two upper-most and between the two lower-most dashed lines, and in Fig. 2c they are above the upper and below the lower dashed lines. Finally, the regions allowed by the *Mantle* asymmetry data in Fig. 1a are between the two dash-dotted lines, in Figs. 1b - 1c they are located to the right of the dash-dotted line; in Figs. 2a - 2c these regions are situated between the two upper-most and between the two lower-most dash-dotted lines. In Figs. 1c and 2c we have shown also the

contour corresponding to the maximal allowed value of A_{D-N}^C at 3 s.d. (the double-thick (black) solid lines). In obtaining the allowed intervals of values of A_{D-N}^N , A_{D-N}^T and A_{D-N}^C at a given C.L. we have added the errors in eqs. (2), (3) and (4) in quadratures. For the *Core* asymmetry this procedure gives the following 1 s.d., 2 s.d. and 3 s.d. allowed intervals of values: $A_{D-N}^C = [-0.081, 0.046]$; $[-0.145, 0.110]$; $[-0.208, 0.173]$. The corresponding intervals of allowed values for the *Night* and *Mantle* asymmetries are: $A_{D-N}^N = [0.031, 0.099]$; $[-0.002, 0.132]$; $[-0.036, 0.166]$, and $A_{D-N}^M = [0.041, 0.113]$; $[0.005, 0.149]$; $[-0.031, 0.185]$.

Since the minimal value of the predicted *Core* D-N asymmetry in the case of the SMA solution is [16] $\sim (-0.03)$ and the lower bound on A_{D-N}^C following from the current Super-Kamiokande data at 1 s.d. is $\min(A_{D-N}^C) \cong (-0.081)$, it is clear that the latter will not play a role in constraining the SMA solution region. The current Super-Kamiokande upper bound on A_{D-N}^C , however, can be used to constrain the MSW SMA solution region.

As Fig. 1a demonstrates, the MSW SMA “conservative” solution region is incompatible with Super-Kamiokande data on the asymmetries A_{D-N}^N or A_{D-N}^T and A_{D-N}^C , eqs. (2) or (4) and (3), including 1 s.d. uncertainties. The same conclusion is practically valid at 1.5 s.d. as well, as Fig. 1b shows: the region compatible with the data on the *Night* and *Core* asymmetries in this case is a tiny “triangle” around the point $\Delta m^2 \cong 4 \times 10^{-6} \text{ eV}^2$ and $\sin^2 2\theta \cong 0.0085$, while the *Mantle* and *Core* asymmetry data leave allowed only a small point-like region at $\Delta m^2 \cong 3.9 \times 10^{-6} \text{ eV}^2$ and $\sin^2 2\theta \cong 0.0091$.

At 2 s.d. a large subregion of the SMA “conservative” solution region is ruled out by the Super-Kamiokande data on the *Core* and *Night* D-N asymmetries: the allowed region in Fig. 1c is located between the thick dashed line corresponding to $\min(A_{D-N}^N) = (-0.002)$ and the dash-dotted line corresponding to $\max(A_{D-N}^C) = 0.110$. The allowed region is even smaller if one uses the data on the *Core* and *Mantle* asymmetries: this is the triangular shaped region to the right of the dash-dotted line and to the left of the thick (black) solid line.

At 3 s.d. level only the data on the *Core* asymmetry constraints the SMA solution region (Fig. 1c): the subregion located to the right of the contour corresponding to $\max(A_{D-N}^C) = 0.173$ (double-thick (black) solid line) is ruled out by these data. Most of the indicated subregion (not to mention the results described above) could not be probed at the indicated C.L. by the earlier Super-Kamiokande data on the asymmetry A_{D-N}^{N5} associated with the night N5 bin data (see, e.g., [5,7–9]).

The combined use of the Super-Kamiokande data on the *Core* and *Mantle* (*Night*) D-N asymmetries is less effective in constraining the MSW LMA solution because the *mantle-core* enhancement effect [20–22] leads [16] to a modest amplification of the *Core* asymmetry with respect to the *Night* (*Mantle*) one in the LMA solution region. The same conclusion is valid for the LOW solution region. The results of our analysis for the LMA and LOW solutions are depicted in Figs. 2a - 2c. It is interesting that, as Fig. 2a shows, large parts of both the LMA and the LOW solution regions are incompatible at 1 s.d. with the Super-Kamiokande data on the asymmetries A_{D-N}^C and A_{D-N}^N : the only allowed regions lie in the narrow bands corresponding to $\Delta m^2 \cong (4.0 - 5.0) \times 10^{-5} \text{ eV}^2$ and to $\Delta m^2 \cong (1.0 - 2.0) \times 10^{-7} \text{ eV}^2$. Even these narrow bands are barely compatible with the allowed values of A_{D-N}^M at 1 s.d. (Fig. 2a).

Similar conclusion is valid if one uses the D-N asymmetry data, eqs. (2) - (4), including the 1.5 s.d. uncertainties, as Fig. 2b shows: the allowed values of A_{D-N}^C , A_{D-N}^M and A_{D-N}^N are compatible with the subregions located between the upper-most dash-dotted and the thick solid lines, and between the lower-most dash-dotted and the thick solid lines. The allowed values of Δm^2 in the case of the LMA solution are confined to the interval $\Delta m^2 \cong (2.2 - 6.5) \times 10^{-5} \text{ eV}^2$. The region of the LOW solution corresponding to $\Delta m^2 \lesssim 9.5 \times 10^{-8} \text{ eV}^2$ is incompatible at the indicated C.L. by the current Super-Kamiokande data on the asymmetry A_{D-N}^M .

These data are considerably less restrictive at 2 s.d. (Fig. 2c): the regions between the upper-most dash-dotted and thick solid lines, and between the lower-most dash-dotted and thick solid lines are compatible with the data. The data on the *Core* asymmetry alone including the 3 s.d. uncertainties (see Fig. 2c) are incompatible with the subregion of the LMA “conservative” solution region located at $\Delta m^2 \lesssim 10^{-5} \text{ eV}^2$.

The solar neutrino data can also be explained assuming that the solar neutrinos undergo MSW transitions into sterile neutrino in the Sun: $\nu_e \rightarrow \nu_s$ (see, e.g., [12,9]). In this case only a SMA solution is compatible with the data. The corresponding solution region obtained (at a given C.L.) using the mean event rate solar neutrino data and the predictions of ref. [6] for the different solar neutrino flux components practically coincides in magnitude and shape with the SMA $\nu_e \rightarrow \nu_{\mu(\tau)}$ solution region, but is shifted by a factor of ~ 1.2 along the Δm^2 axis to smaller values of Δm^2 . The “conservative” $\nu_e \rightarrow \nu_s$ transition solution region extends both in the direction of smaller and larger values of $\sin^2 2\theta$ down to 0.7×10^{-3} and up to 0.4 [9]. The main contribution to the energy-integrated D-N asymmetries in the three Super-Kamiokande event samples of interest comes from the “high” energy tail of the ^8B neutrino spectrum [17]. This is related to the fact the relevant neutrino effective potential difference in the Earth matter in the case of the $\nu_e \rightarrow \nu_s$ transitions is approximately by a factor of 2 smaller than in the case of $\nu_e \rightarrow \nu_{\mu(\tau)}$ transitions [33,17]. As a consequence, the predicted *Core* and *Night (Mantle)* D-N asymmetries for the Super-Kamiokande detector are considerably smaller in the case of the MSW $\nu_e \rightarrow \nu_s$ transition solution than in the case of the MSW SMA $\nu_e \rightarrow \nu_{\mu(\tau)}$ solution. Nevertheless, the current Super-Kamiokande data on the *Core* asymmetry A_{D-N}^C including the 2 s.d. uncertainties, as can be shown, excludes the subregion of the MSW $\nu_e \rightarrow \nu_s$ “conservative” solution region, located, depending on Δm^2 , approximately at $\sin^2 2\theta \gtrsim (0.016 - 0.020)$ (see Fig. 6 in [17]).

III. Conclusions

We have studied the implications of the current Super-Kamiokande data on the *Core*, *Night* and *Mantle* D-N asymmetries, eqs. (2) and (3), for the MSW solutions of the solar neutrino problem. The Super-Kamiokande collaboration published recently for the first time data on the *Core* asymmetry [23]. Performing a very simplified analysis we have found that practically the whole “conservative” region of the MSW SMA $\nu_e \rightarrow \nu_{\mu(\tau)}$ solution in the $\Delta m^2 - \sin^2 2\theta$ plane is incompatible with the indicated data if one includes the 1 s.d. and 1.5 s.d. uncertainties, the only exception in the latter case being a point-like region at $\Delta m^2 \cong 3.9 \times 10^{-6} \text{ eV}^2$ and $\sin^2 2\theta \cong 0.0091$. At 2 s.d. a large subregion of the MSW SMA $\nu_e \rightarrow \nu_{\mu(\tau)}$ solution region is incompatible with the D-N effect data, while at 3 s.d. the data on the *Core* D-N asymmetry *alone* excludes a non-negligible subregion of the indicated solution region (Fig. 1c).

The constraints on the LMA and LOW solution regions from the Super-Kamiokande data on the *Core* and *Night* or *Mantle* D-N asymmetries are somewhat weaker. Nevertheless, both the LMA and the LOW solutions are barely compatible with the *Core* and *Night* asymmetry data at 1 s.d.: the subregions allowed by the indicated data are contained in the narrow bands determined by $\Delta m^2 \cong (4.0 - 5.0) \times 10^{-5} \text{ eV}^2$ and $\Delta m^2 \cong (1.0 - 2.0) \times 10^{-7} \text{ eV}^2$ (Fig. 2a). At 1.5 s.d. these data are incompatible with substantial subregions of both solution regions (Fig. 2b), while at 2 s.d. the LMA solution region at $\Delta m^2 \gtrsim 2.0 \times 10^{-5} \text{ eV}^2$ and the whole LOW solution region are allowed by the Super-Kamiokande *Core* and *Night* or *Mantle* D-N asymmetry data (Fig. 2c).

The current Super-Kamiokande data on the asymmetries A_{D-N}^C and A_{D-N}^N allows to constrain the MSW $\nu_e \rightarrow \nu_s$ “conservative” solution region as well: depending on Δm^2 the subregion located approximately at $\sin^2 2\theta \gtrsim (0.016 - 0.020)$ is ruled out at 2 s.d. by the data.

The simplified analysis we have performed demonstrates, in particular, the remarkable potential

which the data on the *Night* or *Mantle* and especially on the *Core* D-N asymmetry have for testing the MSW $\nu_e \rightarrow \nu_{\mu(\tau)}$ solutions of the solar neutrino problem. As was suggested in [16], these data are particularly effective in testing the MSW SMA $\nu_e \rightarrow \nu_{\mu(\tau)}$ solution. The *Core* D-N asymmetry is strongly enhanced in the case of MSW SMA $\nu_e \rightarrow \nu_{\mu(\tau)}$ solution by the *mantle-core enhancement* effect [20–22]. With the increase of the statistics of the Super-Kamiokande experiment the data on the two indicated D-N asymmetries will allow to probe larger and larger subregions of the SMA solution region. Our results indicate that the data on the *Core* and *Night* or *Mantle* asymmetries can be used to perform rather effective tests of the LMA and LOW $\nu_e \rightarrow \nu_{\mu(\tau)}$ solutions as well. Using these data one can probe and constrain also the MSW $\nu_e \rightarrow \nu_s$ “conservative” solution region. Similarly, one can use the data on the *Core*, *Night* and *Mantle* D-N asymmetries in the charged current event rate in the SNO detector to perform equally effective tests the MSW solutions of the solar neutrino problem [34].

Acknowledgements.

We would like to thank Y. Suzuki and M. Smy for very useful and clarifying correspondence concerning the Super-Kamiokande data on the D-N effect. The work of (S.T.P.) was supported in part by the EC grant ERBFMRX CT96 0090.

REFERENCES

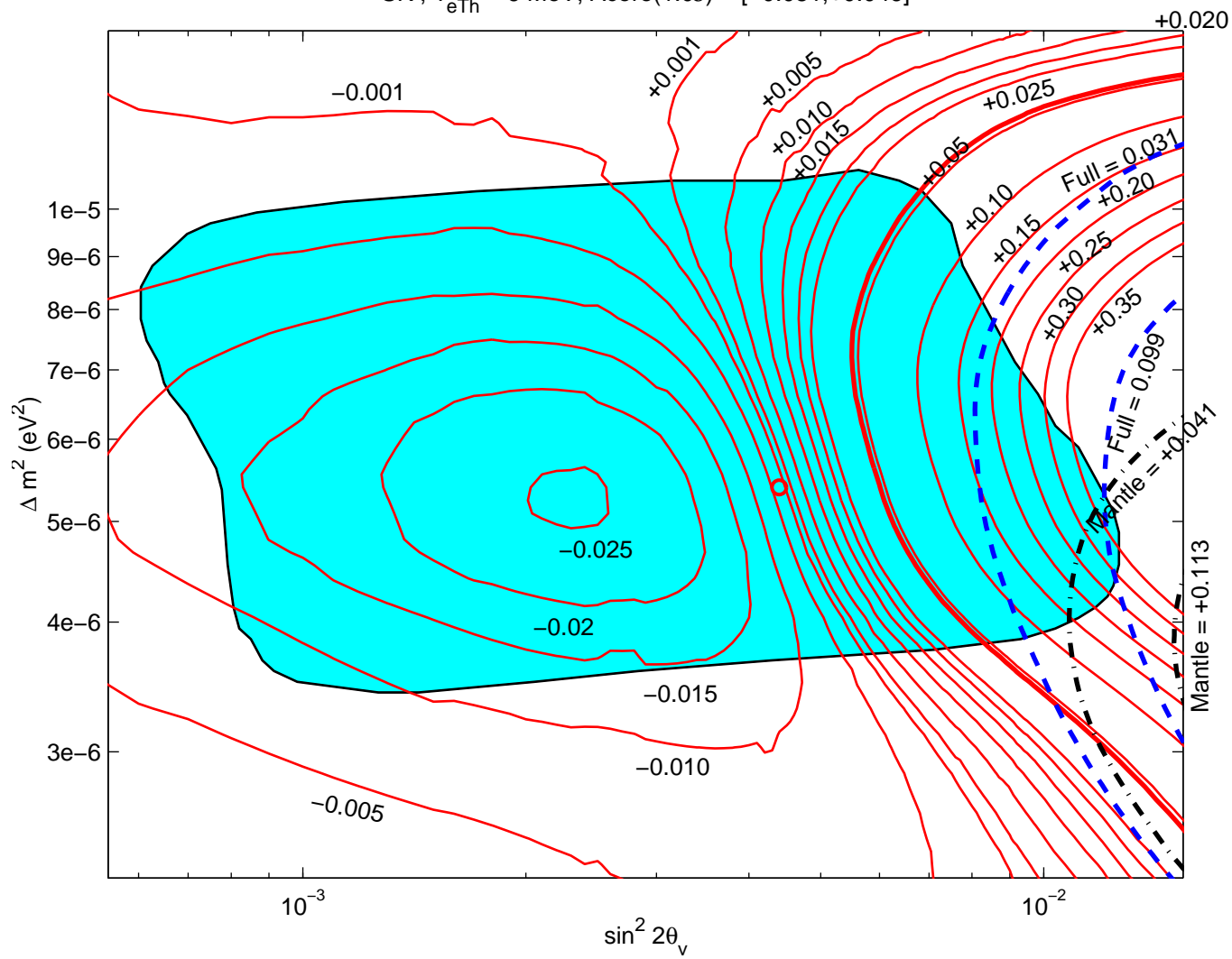
- [1] B. T. Cleveland et al. (Homestake Collaboration), *Astrophys. J.* **496**, 505 (1998).
- [2] Y. Fukuda et al. (Kamiokande Collaboration), *Phys. Rev. Lett.* **77**, 1683 (1996).
- [3] J. N. Abdurashitov et al. (SAGE Collaboration), *Phys. Rev. C* **60**, 055801 (1999).
- [4] W. Hampel et al. (GALLEX Collaboration), *Phys. Lett. B* **447**, 127 (1999).
- [5] Y. Totsuka, Talk given at the XVth Particle And Nuclei International Conference, June 10 - 17, 1999, Uppsala, Sweden; M. Nakahata, Talk given at the VIth International Workshop on Topics in Astroparticle and Underground Physics, September 6 - 10, 1999, Paris, France (transparencies are available at <http://taup99.in2p3.fr/TAUP99/>); Y. Fukuda et al., Super-Kamiokande Coll., *Phys. Rev. Lett.* **82** (1999) 1810.
- [6] J.N. Bahcall, S. Basu and M. Pinsonneault, *Phys. Lett. B* **433**, 1 (1998).
- [7] G.L. Fogli et al., e-Print archive hep-ph/9910387.
- [8] C. Gonzalez-Garcia et al., e-Print archive hep-ph/9906469.
- [9] P.I. Krastev, Talk given at the *Neutrino Summer '99* Workshop, June - July 1999, TH Division, CERN, Geneva, Switzerland (copy of the transparencies is available at <http://lyopsr.in2p3.fr/nufact99/talks/>).
- [10] P.I. Krastev and S.T. Petcov, *Phys. Lett. B* **299**, 99 (1993).
- [11] N. Hata and P. Langacker, *Phys. Rev. D* **50**, 632 (1994).
- [12] P.I. Krastev, Q.Y. Liu and S.T. Petcov, *Phys. Rev. D* **54**, 7057 (1996).
- [13] J.N. Bahcall and P.I. Krastev, *Phys. Lett. B* **436**, 243 (1998).
- [14] A.J. Baltz and J. Weneser, *Phys. Rev. D* **50** (1994) 5971.
- [15] Q.Y. Liu, M. Maris and S.T. Petcov, *Phys. Rev. D* **56**, 5991 (1997).
- [16] M. Maris and S.T. Petcov, *Phys. Rev. D* **56**, 7444 (1997).
- [17] M. Maris and S.T. Petcov, *Phys. Rev. D* **58**, 113008 (1998).
- [18] E. Lisi and D. Montanino, *Phys. Rev. D* **56**, 3081 (1997).
- [19] J.N. Bahcall and P.I. Krastev, *Phys. Rev. C* **56**, 2839 (1997).
- [20] S.T. Petcov, *Phys. Lett. B* **434**, 321 (1998), (E) **B444**, 584 (1998).
- [21] M. Chizhov and S.T. Petcov, *Phys. Rev. Lett.* **83**, 1096 (1999) (hep-ph/9903399).
- [22] M. Chizhov and S.T. Petcov, hep-ph/9903424.
- [23] Y. Suzuki (Super-Kamiokande collaboration), to be published in the Proceedings of the Symposium on Lepton-Photon Interactions at High Energies, August 9 - 15, 1999, Stanford, U.S.A.; M. Vagins, Talk given at the NNN Workshop, February 25 - 27, 2000, UC Irvine, U.S.A. (transparencies are available at <http://www.ps.uci.edu/~nnn/agenda-files.html>).
- [24] J.N. Bahcall, M. Kamionkowski and A. Sirlin, *Phys. Rev. D* **51**, 6146 (1995).
- [25] J.N. Bahcall et al., *Phys. Rev. D* **54**, 411 (1996).
- [26] S.T. Petcov, *Phys. Lett. B* **200B**, 373 (1988).
- [27] P.I. Krastev and S.T. Petcov, *Phys. Lett. B* **207B**, 64 (1988).
- [28] J.N. Bahcall, M.H. Pinsonneault, *Rev. Mod. Phys.* **67**, 781 (1995).
- [29] M. Maris, study performed in 1999, unpublished.
- [30] F.D. Stacey, *Physics of the Earth*, 2nd edition, John Wiley and Sons, London, New York, 1977.
- [31] A.D. Dziewonski and D.L. Anderson, *Physics of the Earth and Planetary Interiors* **25**, 297 (1981).
- [32] R. Jeanloz, *Annu. Rev. Earth Planet. Sci.* **18**, 356 (1990); C.J. Allègre et al., *Earth and Planetary Science Letters* **134**, 515 (1995).
- [33] P. Langacker et al., *Nucl. Phys. B* **282**, 589 (1987).
- [34] M. Maris and S.T. Petcov, Report SISSA 30/2000/EP, March 2000 (e-print archive hep-ph/0003301).

FIGURE CAPTIONS

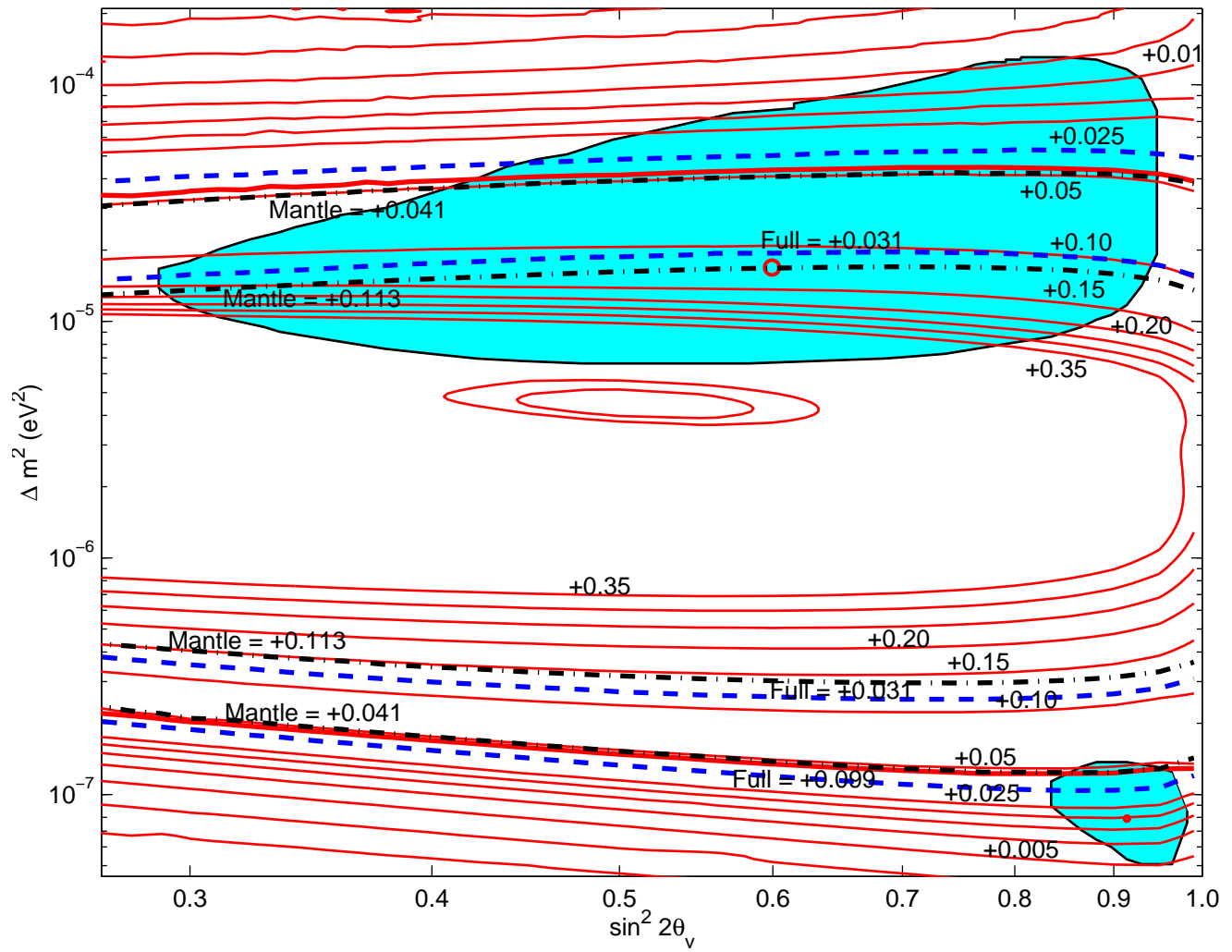
Figs. 1a - 1c. Constraints on the MSW SMA $\nu_e \rightarrow \nu_{\mu(\tau)}$ solution from the Super-Kamiokande data on the *Core*, *Night* and *Mantle* D-N asymmetries, A_{D-N}^C , A_{D-N}^M and A_{D-N}^N , eqs. (3), (4) and (2). The “conservative” SMA solution region [9] is shown in grey color. The thick solid line (the (left) dash-dotted line) corresponds to $\max(A_{D-N}^C)$ ($\min(A_{D-N}^M)$), the dashed lines correspond to the $\min(A_{D-N}^N)$ and $\max(A_{D-N}^N)$, allowed by the Super-Kamiokande data at 1 s.d. (a), 1.5 s.d. (b) and 2 s.d. (c). The double-thick solid line in Fig. 1c corresponds to the 3 s.d. maximal value of A_{D-N}^C allowed by the data. Contours of given *constant Core* D-N asymmetry are also shown (thin solid lines). The region to the left of the thick solid line (double-thick solid line in Fig. 1c) is allowed by the data on A_{D-N}^C (at 3 s.d.), the region between the two dashed lines is allowed by the data on A_{D-N}^N , while the region between the two dash-dotted lines (a) or to the left of the dash-dotted line (b,c) is allowed by the data on A_{D-N}^M .

Figs. 2a - 2c. The same as in figures 1a - 1c for the MSW LMA and LOW $\nu_e \rightarrow \nu_{\mu(\tau)}$ transition solutions. The regions allowed by the *Core* asymmetry data (at 3 s.d.) are located above the upper and below the lower thick solid lines (double-thick solid lines in Fig. 2c). The regions allowed by the *Mantle* asymmetry data are in Figs. 2a - 2c between the two upper and between the two lower dash-dotted lines, while those allowed by the *Night* asymmetry data are in Figs. 2a - 2b between the two upper and between the two lower dashed lines, and in Fig. 2c they are above the upper and below the lower dashed lines.

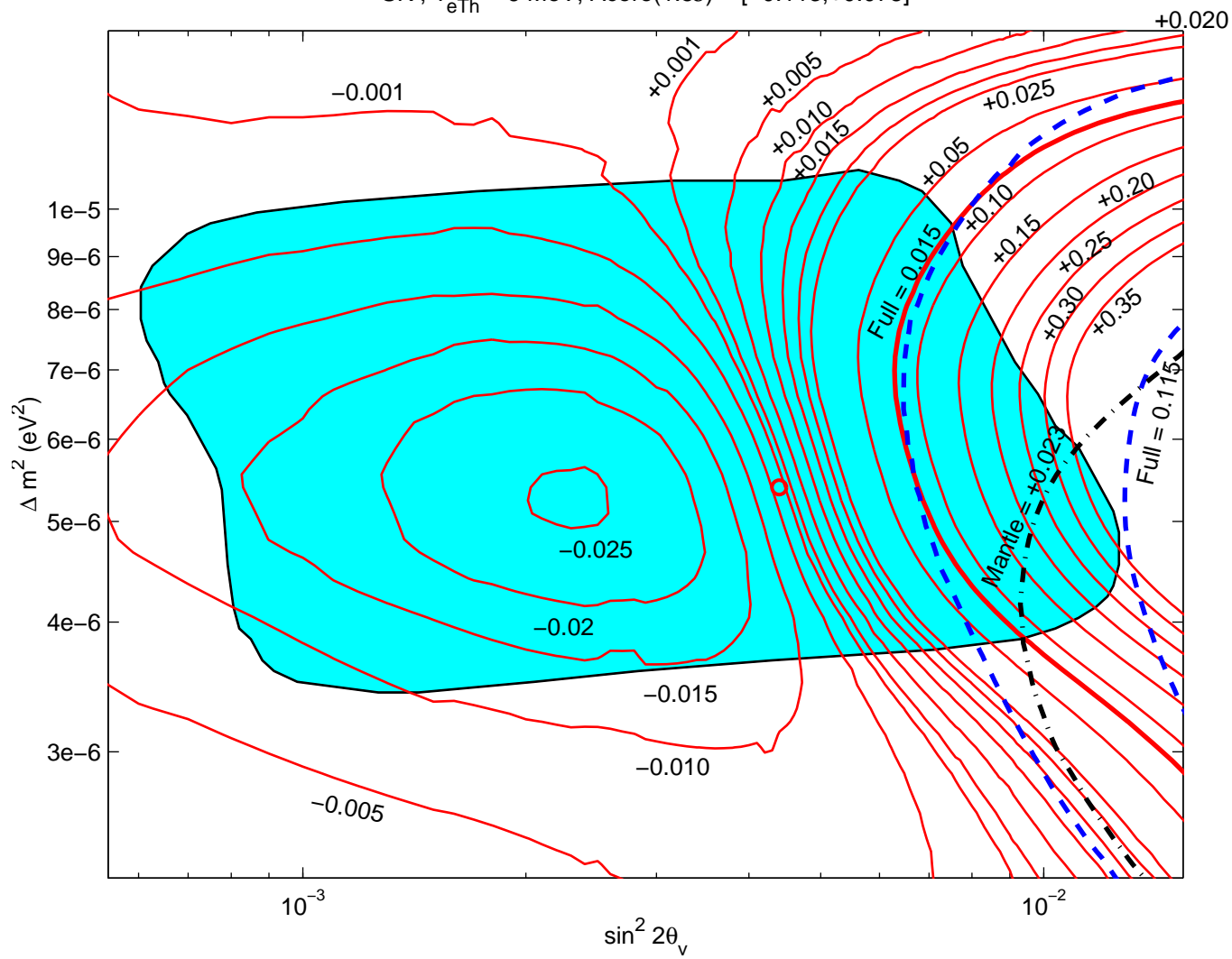
SK , $T_{\text{eTh}} = 6 \text{ MeV}$, $\text{Acore}(1.0\sigma) = [-0.081, +0.046]$



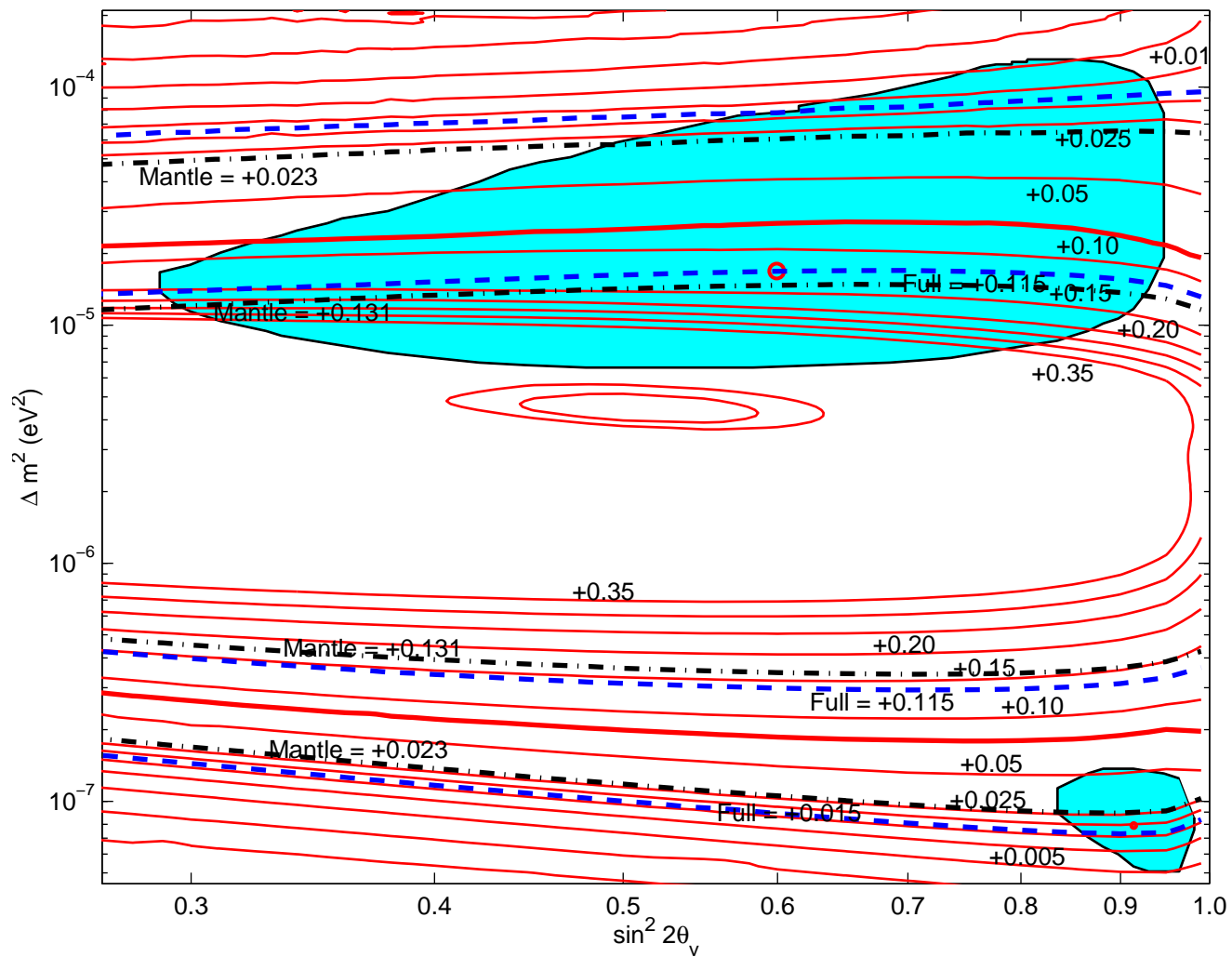
SK , $T_{eTh} = 6$ MeV, $A_{core}(1.0\sigma) = [-0.081, +0.046]$



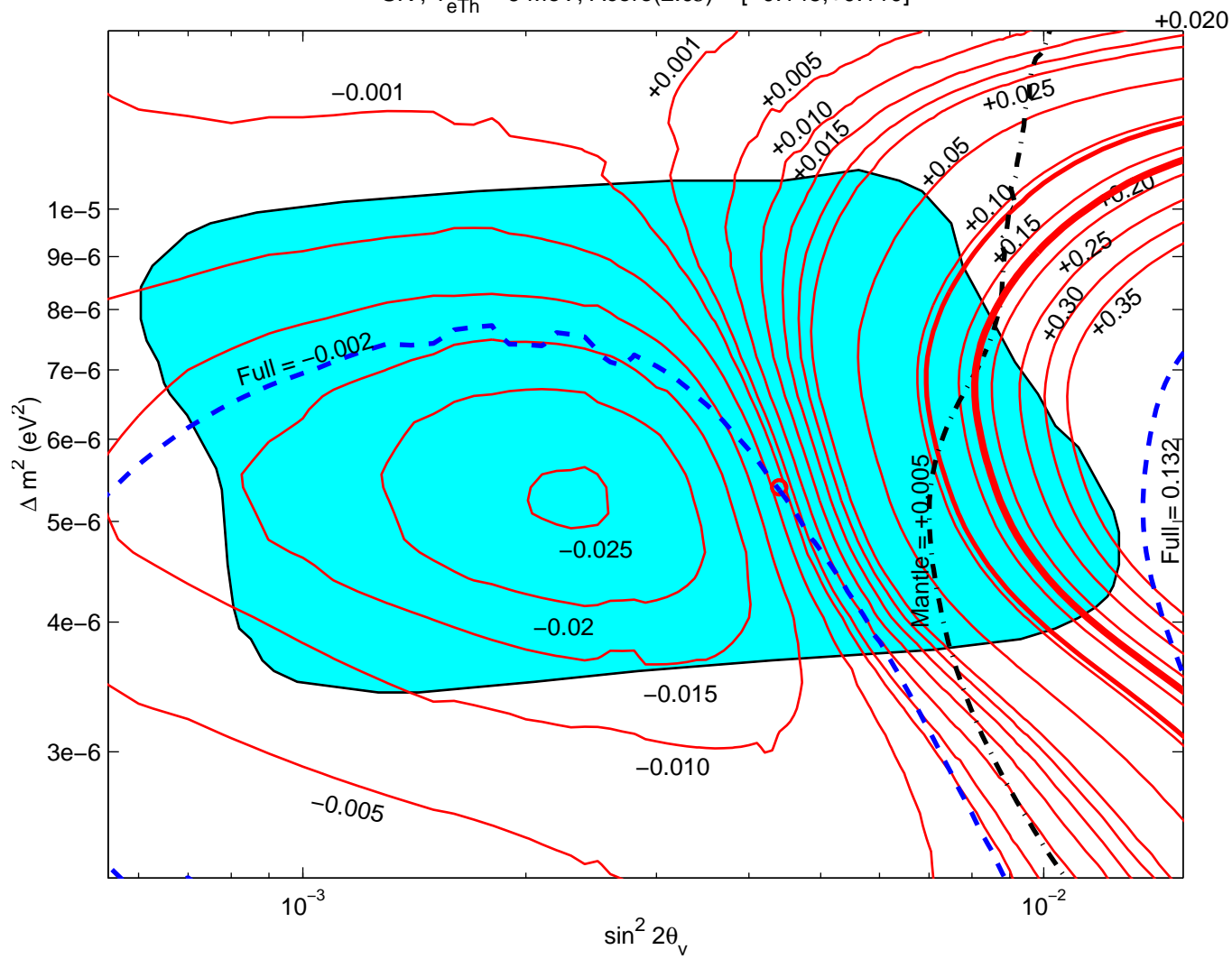
SK , $T_{\text{eTh}} = 6 \text{ MeV}$, $\text{Acore}(1.5\sigma) = [-0.113, +0.078]$



SK , $T_{\text{eTh}} = 6 \text{ MeV}$, $\text{Acore}(1.5\sigma) = [-0.113, +0.078]$



SK , $T_{\text{eTh}} = 6 \text{ MeV}$, $\text{Acore}(2.0\sigma) = [-0.145, +0.110]$



SK , $T_{\text{eTh}} = 6 \text{ MeV}$, $A_{\text{core}}(2.0\sigma) = [-0.145, +0.110]$

